



# University of HUDDERSFIELD

## University of Huddersfield Repository

Anyakwo, Arthur, Pislaru, Crinela, Ball, Andrew and Gu, Fengshou

A Novel Approach To Modelling And Simulation Of The Dynamic Behaviour Of The Wheel-Rail Interface

### Original Citation

Anyakwo, Arthur, Pislaru, Crinela, Ball, Andrew and Gu, Fengshou (2011) A Novel Approach To Modelling And Simulation Of The Dynamic Behaviour Of The Wheel-Rail Interface. In: Proceedings of the 17th International Conference on Automation & Computing. Chinese Automation and Computing Society, Huddersfield. ISBN 978-1-86218-098-7

This version is available at <http://eprints.hud.ac.uk/id/eprint/11492/>

The University Repository is a digital collection of the research output of the University, available on Open Access. Copyright and Moral Rights for the items on this site are retained by the individual author and/or other copyright owners. Users may access full items free of charge; copies of full text items generally can be reproduced, displayed or performed and given to third parties in any format or medium for personal research or study, educational or not-for-profit purposes without prior permission or charge, provided:

- The authors, title and full bibliographic details is credited in any copy;
- A hyperlink and/or URL is included for the original metadata page; and
- The content is not changed in any way.

For more information, including our policy and submission procedure, please contact the Repository Team at: [E.mailbox@hud.ac.uk](mailto:E.mailbox@hud.ac.uk).

<http://eprints.hud.ac.uk/>

## A NOVEL APPROACH TO MODELLING AND SIMULATION OF THE DYNAMIC BEHAVIOUR OF THE WHEEL-RAIL INTERFACE

Arthur Anyakwo, Crinela Pislaru, Andrew Ball, Fengshou Gu  
University of Huddersfield  
Diagnostics Engineering Research Centre  
Queensgate, Huddersfield, HD1 3DH  
arthur.anyakwo@hud.ac.uk

**Abstract**— This paper presents a novel approach to modelling and simulation of the dynamic behaviour of rail-wheel interface. The proposed dynamic wheel-rail contact model comprises wheel-rail geometry and efficient solutions for normal and tangential contact problems. This two-degree of freedom model takes into account the lateral displacement of the wheelset and the yaw angle. Single wheel tread rail contact was considered for all simulations and Kalker's linear theory and heuristic non-linear creep models were employed. The second order differential equations are reduced to first order and the forward velocity of the wheelset is increased until the wheelset becomes unstable. A comprehensive study of the wheelset lateral stability is performed and is relatively easy to use since no mathematical approach is required to estimate the critical velocity of the dynamic wheel-rail contact model.

This novel approach to modelling and simulation of the dynamic behaviour of rail-wheel interface will be useful in the development of intelligent infrastructure diagnostic and condition monitoring systems. The automated detection of the state of the track will allow informed decision making on asset management actions – especially in maintenance and renewals activities.

**Keywords:** modelling; simulation; condition monitoring; systems engineering; wheel-rail contact

### NOMENCLATURE

$R_0$  = Nominal rolling radius of the wheel (460mm)  
 $R_l$  = left wheel rolling radius (mm)  
 $R_r$  = Right wheel rolling radius (mm)  
 $R_{rail}$  = Rail radius (79.37 mm)  
 $a$  = Half length of the semi-axes of c  
in the rolling direction (mm)  
 $b$  = Half length of the semi-axis of contact  
patch in the lateral direction (mm).  
 $I_z$  = Moment of Inertia of the wheelset ( $700 \times 10^6 \text{ kg}\cdot\text{mm}^2$ )  
 $K_{py}$  = Lateral suspension stiffness ( $3.86 \times 10^3 \text{ N/mm}$ )  
 $K_{px}$  = Longitudinal spring stiffness (850 N/mm)  
 $C_{py}$  = Lateral damper coefficient (8 Ns/mm)  
 $C_{px}$  = Longitudinal damper coefficient (100 Ns/mm)  
 $f_{11}$  = Longitudinal linear creep coefficient ( $8.06 \times 10^6 \text{ N}$ )  
 $f_{22}$  = Lateral linear creep coefficient ( $8.09 \times 10^6 \text{ N}$ )  
 $f_{23}$  = Lateral/spin linear creep coefficient ( $2.2 \times 10^7 \text{ N}\cdot\text{mm}$ )  
 $f_{33}$  = Spin linear creep coefficient ( $1.27 \times 10^7 \text{ Nmm}^2$ )  
 $m$  = Mass of the wheelset (1250kg)  
 $W$  = Axle load (110,000N)  
 $v_x$  = longitudinal creepage  
 $v_y$  = lateral creepage  
 $v_{spin}$  = Spin creepage  
 $l_0$  = Half wheel axle length in central position (742.9mm)

$G$  = Shear Modulus of rigidity =  $80 \times 10^3 \text{ MPA}$   
 $C_{11}$  = Longitudinal creep coefficient  
 $C_{22}$  = Lateral creep coefficient  
 $C_{23}$  = Lateral/spin creep coefficient  
 $C_{33}$  = Spin linear coefficient  
 $d$  = Half distance between the two springs (900mm)  
 $l_0$  = Half wheelset axle distance (742.9mm)  
 $\dot{\phi}$  = Roll velocity

### I. INTRODUCTION

The lateral stability of the wheelset affects the dynamic motion of the railway vehicle. This phenomenon depends on the wheel-rail contact model, wheel-rail profile design, hunting, critical velocity and creep contact forces acting on the contact patch. Hertz theory was applied to solve wheel-rail contact problems [1]. Hertz model runs very fast in real time and is thus used in most railway vehicle dynamic simulations. However for rapidly changing contacts with time and with increased normal contact forces, Hertz model is not suitable since in these situations the contact region becomes conformal. Semi-Hertzian method [2-3] was developed to cater for the variations and increase in the normal contact forces acting on the wheel-rail interface. It uses the geometric intersection of two solids in contact region to find out the shape of the contact patch. Kalker, [4] proposed the exact theory of the wheel-rail contact model by developing a robust algorithm called CONTACT. This model requires so much computation power since the contact patch is discretized into stripes before the tangential creep forces are calculated. Finite Element Method (FEM) [5] was used to model the dynamics of the wheel-rail interface. Due to the enormous computational time required to implement FEM methods, it rarely used for railway vehicle dynamic simulations.

The tangential creep forces play a vital role in wheel-rail rolling theory. Carter solved the 2-Dimensional problem of wheel-rail contact rolling theory using a locomotive wheel and a cylindrical rail [6]. He maintained the fact that the tangential creep forces must not exceed the Coulombs maximum limit. Johnson and Vermeulen extended Carter's theory to 3-dimensional case to include the two smooth half rolling surfaces without spin. Carter's model considered only the relationship between the longitudinal creepage and the tangential forces on the contact patch region. Kalker [7] proposed the linear theory for determining the tangential forces acting on the contact patch. A new Heuristic non-linear model [8-9]

developed by Shen for limiting the tangential forces is discussed. Several dynamic models have been developed for wheel-rail interface using the wheel-rail profile geometry. A parametric 3-dimensional wheel-rail contact model was developed to model the dynamics of the wheel-rail contact model [10]. Wickens [11] studied the effect on hunting on a railway vehicle on a straight track. He observed that hunting motion occurs when the critical velocity of the wheelset exceeds the maximum required speed limit of the designed for its operation. Finally a new model was developed to study the dynamic interaction of the wheel-rail contact on a curved track [12]. This study showed that the lateral and longitudinal stiffness has significant effect on critical velocity of the railway vehicle.

In this paper a two dimensional wheel-rail contact model is modeled. Hertz contact model is used to get the contact patch size dimensions and then the Heuristic nonlinear model is applied to limit the creep contact forces. The lateral stability of the wheelset is investigated by solving the system of non-linear equations of the model using Runge-Kutta's method. The lateral stability of the wheelset is then investigated by increasing the forward velocity of the wheelset until it becomes unstable. The proposed model contains; wheel-rail contact geometry, normal and tangential contact problems and equations for describing the dynamic equation (see Fig. 1).

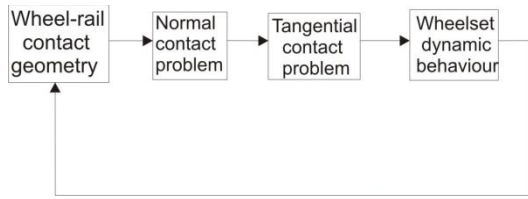


Fig. 1 Dynamic Wheel-rail Contact Model

## II. WHEEL-RAIL CONTACT GEOMETRY

A new conical wheel profile with wheel tread taper 1:20 is used to model the dynamic wheel-rail contact model. A BS 113A rail profile is also used for the model of the rail-profile. The nominal rolling radius  $R_o$  of the wheelset is 460mm while the rail radius  $R_{rail}$  in contact point range is 79.37mm as shown in Fig. 2. This is the contact point range for the wheelset on the track.

Assuming that the yaw angle of the wheelset is very small and can be neglected, the 2-Dimensional model of the wheel-rail contact geometry considering the vertical displacement  $u_z$  and the lateral displacement  $u_y$  is modeled (see Fig. 3).

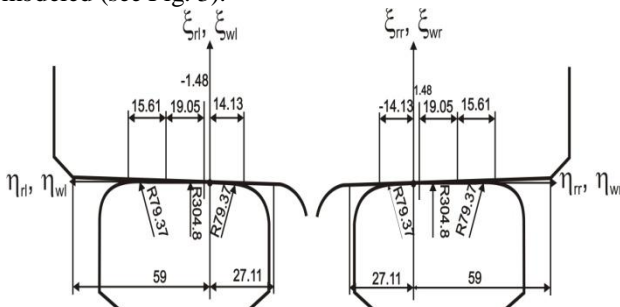


Fig. 2 Wheel-rail contact geometry

The railway track is considered to be rigid and there is no cant applied at both rails. When the wheelset is in central position, the angle made by the horizontal plane is  $\delta_{wr}$  for the right wheel and  $\delta_{wl}$  for the left wheel. Similarly, the co-ordinate of point A at central position with respect to the wheelset frame is  $(l_o, -R_o)$ . When the wheelset is displaced laterally from its central position to the right (as shown in Fig. 3) the rail contact slope formed by the new wheel rail contact point B from A for right wheel profile is  $\delta_{rr}$ . It is a function of the roll angle  $\phi$  and the wheel contact slope  $\delta_{wr}$ . The rolling radius for the right and left wheel tread becomes  $R_r$  and  $R_l$ . The previous wheel-rail contact point on the wheel is now contact point C (see Fig. 3).

The wheel-rail co-ordinates are defined (see Fig. 2) as follows

- $\eta_{wr}$  = Right wheel co-ordinate (lateral direction)
- $\eta_{rr}$  = Right rail co-ordinate (lateral direction)
- $\xi_{wr}$  = Right wheel co-ordinate (vertical direction)
- $\xi_{rr}$  = Right rail co-ordinate (vertical direction)
- $u_z$  = Vertical displacement
- $u_y$  = Lateral displacement

The lateral distance between point A and C is

$$\Delta Y_c = Y_c - l_o = (u_y + l_o) \cos \phi + (u_z - R_o) \sin \phi - l_o \quad (1)$$

Similarly, the total vertical distance from point A to C is

$$\Delta Z_c = Z_c - (-R_o) = (u_y + l_o) \sin \phi + (u_z - R_o) \cos \phi + R_o \quad (2)$$

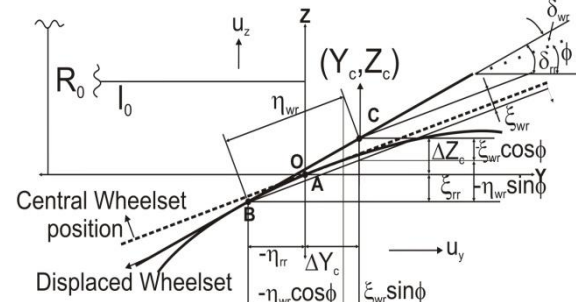


Fig. 3 Right wheel rail geometry

The total lateral distance between point B and C is

$$\eta_{wr} \cos \phi + \xi_{wr} \sin \phi - (-\Delta Y_c + \eta_{rr}) = 0 \quad (3)$$

Also, the vertical distance between point B and C is

$$-\eta_{wr} \sin \phi + \xi_{wr} \cos \phi - (\Delta Z_c + \xi_{rr}) = 0 \quad (4)$$

where  $Z_c$  and  $Y_c$  are the vertical and lateral co-ordinates at point C.

For small roll angles  $\cos \phi = 1$ , and  $\sin \phi = 0$ , Eq. 3 and Eqn. 4 simplifies to

$$u_y + R_o \phi + \xi_{wr} \phi - u_z \phi + \eta_{wr} - \eta_{rr} = 0 \quad (5)$$

$$u_z + l_o \phi + \eta_{wr} \phi + u_y \phi + \xi_{wr} - \xi_{rr} = 0 \quad (6)$$

The right rail contact slope  $\delta_{rr}$  (see Fig. 3) is

$$\delta_{rr} - \delta_{wr} - \phi \quad (7)$$

Similarly the equations for the left hand wheel-rail contact geometry are

$$u_y + R_o \phi + \xi_{wl} \phi - u_z \phi + \eta_{rl} - \eta_{wl} = 0 \quad (8)$$

$$u_z - l_0 \phi + u_y \phi - \eta_{wl} \phi + \xi_{rl} - \xi_{wl} = 0 \quad (9)$$

$$\delta_{rl} - \delta_{wl} + \phi \quad (10)$$

Assuming that the contact points are constrained between the region of  $-14.13\text{mm} < \eta_{wr} < 1.48\text{mm}$  and  $-1.48\text{mm} < \eta_{wl} < 14.13\text{mm}$  for the right and left wheel profile, then the wheel profile equations is

$$\xi_{wr} - 0.05\eta_{wr} = 0 \quad (11)$$

$$\xi_{wl} + 0.05\eta_{wl} = 0 \quad (12)$$

The BS 113A rail profile is made up of three main curves with rail radius of 79.37mm, 304.8mm, 79.37 mm (see Fig. 2). The equation of the curves for the region  $-14.13\text{mm} < \eta_{rr} < 1.48\text{mm}$ , right rail contact point region and  $-1.48\text{mm} < \eta_{rl} < 14.13\text{mm}$ , left rail contact point region can be defined as follows;

$$\xi_{rr} = -79.27 + (79.37^2 - (\eta_{rr} - 3.96)^2)^{1/2} \quad (13)$$

$$\xi_{rl} = -79.27 + (79.37^2 - (\eta_{rl} + 3.96)^2)^{1/2} \quad (14)$$

The wheel contact slope is defined as

$$\delta_{wr} = d\xi_{wr} / d\eta_{wr} = 0.05 \quad (15)$$

$$\delta_{wl} = d\xi_{wl} / d\eta_{wl} = -0.05 \quad (16)$$

$$\delta_{rr} = d\xi_{rr} / d\eta_{rr} = (\eta_{rr} - 3.96) / (79.37^2 - (\eta_{rr} - 3.96)^2)^{1/2} \quad (17)$$

$$\delta_{rl} = d\xi_{rl} / d\eta_{rl} = (\eta_{rl} + 3.96) / (79.37^2 - (\eta_{rl} + 3.96)^2)^{1/2} \quad (18)$$

Equations (5) to (18) can be solved synchronously taking  $u_y$  as the input variable using Newton's method which is discussed next.

#### A. Numerical Solution (Newton Raphson Method)

Several methods exist for solving non-linear multi-dimensional equations. The two most common methods include the Newton Raphson's method and the Quasi-Newton method. Newton Raphson method is a numerical method for solving simultaneous non-linear equations. It provides quadratic convergence of the solutions provided the initial conditions are close to the actual solution [15]. The algorithm for implementing this method is

$$x_{k+1} = x_k - J^{-1} f(x_k) \quad (19)$$

where

$J^{-1}$  = Inverse Jacobian matrix of  $f(x_k)$

$x_k$  = initial guess used as the starting point for iterations

$x_{k+1}$  = the new guess

The Newton Raphson algorithm terminates only when the function  $f(x)$  is close to zero. The value of  $x$  at that point is obtained as the solution to the equation. For application to solving the wheel-rail contact geometry equations, Newton Raphson's method is less efficient since for every lateral displacement input  $u_y$ , the initial conditions must be guessed to ensure quick convergence to the solution. A better method for solving these equations is the Quasi-Newton method [15].

#### B. Quasi Newton Method

Identify applicable sponsor/s here. (sponsors)

The Quasi-Newton method is an optimization technique that can be used to solve a system of non-linear differential equations. In Newton-Raphson's method, the Jacobian matrix had to be computed in every iteration but with the Quasi-Newton method, a single Jacobian matrix is determined and thus used for iteration. In Matlab, the function `fsolve` is used to solve a set of simultaneous non-linear equations using Quasi-Newton's theory of the form

$$f(x) = 0; \quad (20)$$

The algorithms implemented in `fsolve` function are Gauss-Newton method, Levenberg-Marquardt method and the Trust-Region-Reflective method [14]

The syntax used for implementation in Matlab is [14];

$$x = \text{fsolve}(\text{function}, x0, \text{options}) \quad (21)$$

where

$x$  = solution of the equation in vector form

$\text{function}$  = function file containing the set of non-linear simultaneous equations

$x0$  = the initial condition of  $x$

$\text{options}$  = optimization options used for simulations.

Writing the wheel-rail geometry equations into a function file and solving using initial conditions  $x0$  equal to zeros all through, the wheel-rail co-ordinates converged easily to the solution.

For the dynamic wheel-rail contact model, the two most important parameters that are required are the contact angle and the rolling radius difference of the curve.

The contact angle for the left and right wheel-rail geometry defined in Eqn. (7) and (10) would be used for the dynamic model simulation. The rail contact angle plot for the left/right wheel contact is shown below

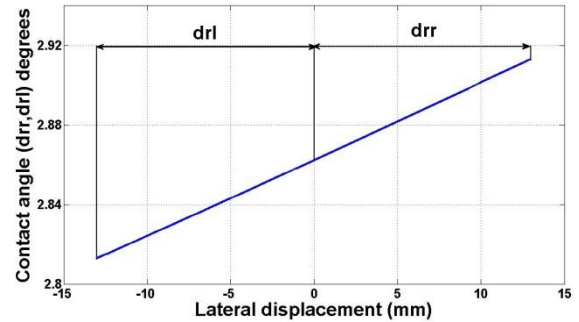


Fig. 5 Contact angle (left and right wheel-rail contact)

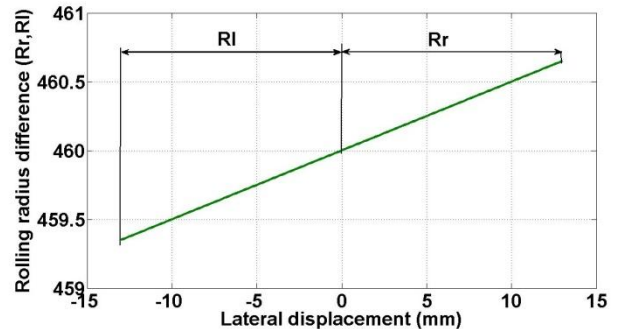


Fig. 6 Rolling radius difference (left and right wheel rail contact)

Fig. 6 shows the Rolling radius difference of the wheelset derived from the left and right vertical wheel co-ordinates  $\xi_{wr}$  and  $\xi_{wl}$  as follows

$$R_r = R_0 + \xi_{wr} \quad (22)$$

$$R_l = R_0 - \xi_{wl} \quad (23)$$

The flangeway clearance for this model is 13mm. Single wheel-rail contact simulations is considered in the wheel tread region for the left and right wheel.

### III THE NORMAL CONTACT PROBLEM

For an applied load on a wheel-rail interface, Normal contact forces develop on the contact patch depending on the total vertical force applied and the contact angle of the wheel-rail contact formed as a result of the lateral displacement  $y$  of the wheelset during motion (see Fig. 7).

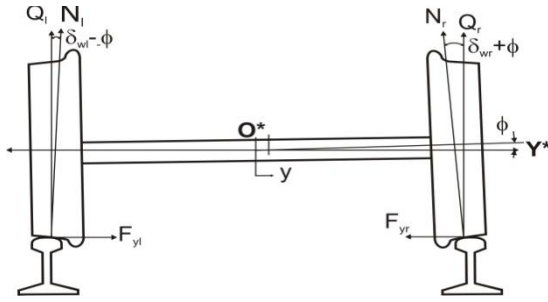


Fig. 7 Vertical and Normal Contact forces acting

The normal contact forces acting on the left and right wheel in static equilibrium is  $Q_r$  and  $Q_l$  given as

$$N_l \cos(\delta_{wl} - \phi) = Q_l \quad (24)$$

$$N_r \cos(\delta_{wr} + \phi) = Q_r \quad (25)$$

The lateral forces  $F_{yr}$  and  $F_{yl}$  can be resolved as follows assuming small roll angles

$$-N_l \sin(\delta_{wl} - \phi) = F_{yr} \quad (26)$$

$$N_r \sin(\delta_{wr} - \phi) = F_{yl} \quad (27)$$

The total lateral force acting on the contact patch is

$$F_{yr} - F_{yl} = Q_l \tan(\delta_{wr} - \phi) - Q_r \tan(\delta_{wl} + \phi) \quad (28)$$

For small contact angles

$$G_r = F_{yr} - F_{yl} = W\phi \quad (29)$$

$G_r$  is the gravitational force. The Gravitational force restores the wheelset back to its central position when it is displaced in the lateral direction.

#### A. Hertz Contact Model

Hertz contact theory predicts the size of the contact patch using the following formulae;

$$ab = mn \left[ \frac{3(1-u^2)}{2E(A+B)} N \right]^{2/3} \quad (30)$$

where  $m$  and  $n$  are the Hertz elliptical constants [2],  $N$  is the normal force(left and right wheel-rail) acting on the contact patch and  $A$  and  $B$  are the relative curvatures given as

$$A = \frac{1}{R}, \quad B = \frac{1}{R_{rail}} \quad (31)$$

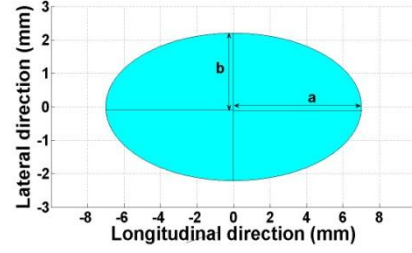


Fig. 8 Elliptical Contact Patch for 0mm lateral displacement (Left/Right wheel-rail contact)

$R$  is the Nominal rolling radius at left and right wheel in the central position or the rolling radii of the left and right wheel as a result of lateral displacement.  $R_{rail}$  is the radius of the rail. In Fig. 8, the Elliptical contact patch for the wheel-rail contact model is shown with values  $a = 7.0045\text{mm}$  and  $b = 2.20245\text{mm}$ . Poisson's ratio ( $\nu = 0.3$ ) and Young Modulus ( $E = 210000\text{MPa}$ ).

### IV TANGENTIAL CONTACT PROBLEM

The tangential contact problem resolves the tangential creep forces acting on the contact patch. A deviation from pure rolling motion of the wheelset is caused by acceleration, traction, braking and the presence of lateral forces acting on the wheel-rail interface. Creepages are thus formed as a result and can be represented as

$$v_x = \frac{v_{1x} - v_{2x}}{v} \text{ (longitudinal creepage)} \quad (32)$$

$$v_y = \frac{v_{1y} - v_{2y}}{v} \text{ (Lateral creepage)} \quad (33)$$

$$v_{spin} = \frac{\Omega_1 - \Omega_2}{v} \text{ (Spin creepage)} \quad (34)$$

where  $v$  is velocity and  $v_{2x}$ ,  $v_{2y}$ ,  $\Omega_2$  are the real velocities while  $v_{1x}$ ,  $v_{1y}$ ,  $\Omega_1$  are the pure rolling velocities of the wheels in the absence of creep. The longitudinal creepages at (right and left) wheel-rail contact

$$v_{xr} = \frac{v(1 - R_r/R_0) - l_0\dot{\psi}}{v}, v_{xl} = \frac{v(1 - R_l/R_0) + l_0\dot{\psi}}{v} \quad (35)$$

The lateral creepages at the right and left wheel-rail contact

$$v_{yr} = (v^{-1}\dot{y} - \psi)(R_r/R_0) + v^{-1}\dot{\phi} \quad (36)$$

$$v_{yl} = (v^{-1}\dot{y} - \psi)(R_l/R_0) + v^{-1}\dot{\phi} \quad (37)$$

The spin creepages at the right and left wheel-rail contact is

$$v_{spinr} = (v^{-1}\dot{\psi} - \lambda/R_0) \quad (38)$$

$$v_{spintl} = (v^{-1}\dot{\psi} + \lambda/R_0) \quad (39)$$



### A. Kalker's Linear Theory

Kalker established a linear relationship between the developed creepages at the contact patch and the creep forces [7]. The maximum creep forces as determined by Kalker are as follows

Longitudinal creep force

$$F_{xr} = -f_{11}^v v_{xr} \quad (40)$$

$$F_{xl} = -f_{11}^v v_{xl} \quad (41)$$

Lateral creep force

$$F_{yr} = -f_{22}^v v_{yr} - f_{23}^v v_{spinr} \quad (42)$$

$$F_{yl} = -f_{22}^v v_{yl} - f_{23}^v v_{spinl} \quad (43)$$

Spin creep moment

$$M_{zr} = f_{23}^v v_{yr} - f_{33}^v v_{spinr} \quad (44)$$

$$M_{zl} = f_{23}^v v_{yl} - f_{33}^v v_{spinl} \quad (45)$$

where  $f_{11}, f_{22}, f_{23}, f_{33}$  are the linear creep coefficients given computed as

$$f_{11} = GabC_{11} \quad (46)$$

$$f_{22} = GabC_{22} \quad (47)$$

$$f_{23} = G(ab)^{1.5} C_{23} \quad (48)$$

$$f_{33} = G(ab)^2 C_{33} \quad (49)$$

$C_{11}, C_{22}, C_{23}, C_{33}$  are the creep coefficients tabulated by Kalker [6] and  $G$  is the Shear modulus of rigidity of steel.

### B Heuristic Non-linear Model

The Heuristic non-linear creep model was developed by Shen and White [8] to cater for the non-linearities in the wheel-rail geometry, adhesion limits on the creep force-creepage relationship and the spin creepage effect. The creep forces developed by Kalker's linear theory are limited for high creepages by a saturation constant 'a' developed as follows;

$$a = \begin{cases} \alpha^{-1}(\alpha - 3^{-1}\alpha^2 + 27^{-1}\alpha^3), & \alpha \leq 3 \\ \alpha^{-1}, & \alpha > 3 \end{cases} \quad (50)$$

$$\text{where } \alpha = \frac{\sqrt{(F_{xi})^2 + (F_{yj})^2}}{\mu N} \quad (i = r, l \quad j = r, l) \quad (51)$$

$\alpha$  = unlimited normalized creep ratio

The reduced creep forces now become

$$F_x^r = aF_x \quad (52)$$

$$F_y^r = aF_y \quad (53)$$

$$M_z^r = aM_z \quad (54)$$

### V WHEELSET DYNAMIC BEHAVIOUR

The dynamic behaviour of the wheelset is studied by summing the total forces acting on the wheelset and then applying Newton's law. In this paper the suspended wheelset is used which includes the primary suspensions

in the longitudinal and lateral direction. The top view of the suspended wheelset is shown below where  $x$  is the rolling direction and  $y$  is the lateral direction.

The suspension forces in the lateral direction and longitudinal direction can be resolved as follows (see Fig. 9)

$$F_{susp} = -2K_{py}y - 2C_{py}\dot{y} \quad (55)$$

$$M_{susp} = -2K_{px}d^2\psi - 2C_{px}d^2\dot{\psi} \quad (56)$$

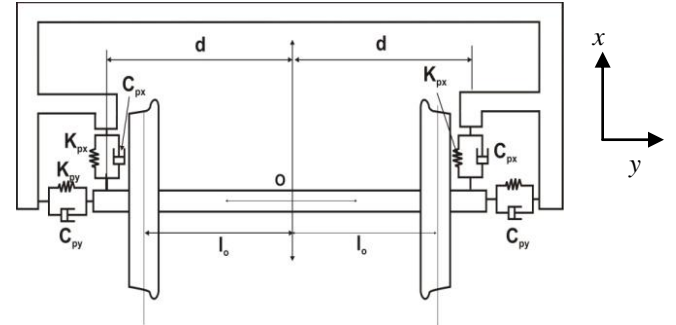


Fig. 9 Top view (Suspended Wheelset diagram)

The equations of motion of the can be derived by combining Eqns. (40 – 45, 55-56) to arrive at the Kalker linear model. For the Heuristic nonlinear model, Eqns. (52-54) is used to replace the maximum creep forces computed in Eqns. (40 – 45). Neglecting the effect of the gyroscopic wheel moment, the two degree of freedom equations of motion comprising of the lateral displacement  $y$ , and the yaw angle  $\psi$  are defined as follows

$$\begin{aligned} m\ddot{y} &= -2f_{22}^v v^{-1} (1 + l_0^{-1} R_0 \lambda + 2C_{py}) \dot{y} - 2f_{33}^v v^{-1} \dot{\psi} \\ &\quad - (2K_{py} + l_0^{-1} W\lambda\lambda) + 2f_{22}^v \psi = 0 \end{aligned} \quad (57)$$

The yaw rotation equation of motion is

$$\begin{aligned} I_z \ddot{\psi} &= 2f_{23}^v v^{-1} (1 + l_0^{-1} R_0 \lambda - I_y \lambda v R_0 l_0) \dot{y} - \\ &\quad - 2(f_{11} + l_0^2 f_{11}^2) v + 2 * C_{px} d^2 \dot{\psi} - 2f_{11} l_0 \lambda / R_0 \\ &\quad - (2f_{22} + 2K_{px} d^2 + W\lambda\lambda) \psi = 0 \end{aligned} \quad (58)$$

### A. Equations of Motion

The equations of motion of the suspended wheelset Eqn. (50)-(51) is can reduced to a system of first order differential equations;

$$\dot{x}(t) = f[x(t)] \quad (59)$$

where  $x(t)$  is a 4 x 1 state vector variable.

### VI SIMULATED RESULTS

The ODE45 function in MATLAB implements Runge Kutta 4<sup>th</sup> order method with variable time step for computational efficiency [14]. It solves initial value problems of the form

$$\dot{x}(t) = f(t, x), \quad x(t_0) = x_0 \quad (60)$$

where  $x$  is a state vector of the dependent variables and  $t$  is the independent variable [14].

Applying Ode45 function to solving the equations of motion, the syntax used is

[t,x] = ode45 (@fun, tspan, initialconditions)  
 Where fun = function file contain the reduced first order differential equations of motion for the system  
 tspan = time span for simulation (30 seconds)  
 initialconditions = initials conditions required for simulation of the dynamic wheel-rail contact model.

The state variables used for simulation is  
 $x(1)$  = Lateral displacement (Initial condition = 5mm)  
 $x(2)$  = Yaw angle (Initial condition = 0)  
 $x(3)$  = Lateral velocity (Initial condition = 0)  
 $x(4)$  = Yaw velocity (Initial condition = 0)

Further details on the use of Ode45 function can be found in [14]. Fig. 10 and Fig.11 shows Kalker linear Model and the Heuristic Non-linear Model results for various forward velocity inputs. Increasing the forward velocity of the wheelset from 5m/s (5000mm/s) to 40m/s leads to increasing amplitude peaks until the critical velocity is reached. For Kalker's linear model, the critical velocity just before flange contact is 40m/s while for the Heuristic Non-linear model, the critical velocity just before wheel flange contact is 35m/s. It can be readily noted that the critical hunting speeds of the linear model is generally slightly higher than the critical speed for the Heuristic non-linear model. Therefore increase in the forward speed of the wheelset leads to lateral instability and hunting. In most real situations the gravitational forces act as a restoring force to limit these increasing lateral oscillations.

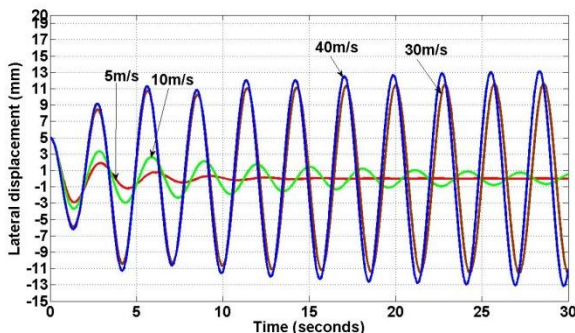


Fig. 10 Lateral displacement of the wheelset for initial velocity 10, 30, 40m/s (Kalker's linear Model)

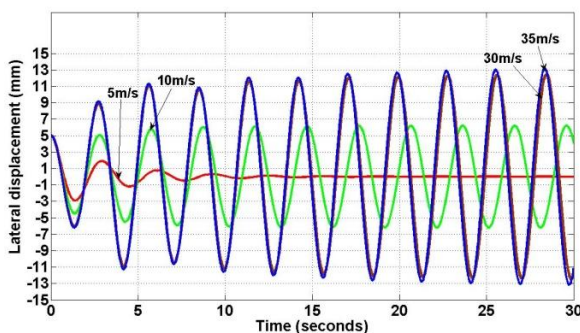


Fig. 11 Lateral displacement of the Wheelset for initial velocity 10, 30, 40m/s (Heuristic Non-linear Model)

## VII

## CONCLUSIONS

In this paper, a new dynamic wheel-rail contact model was developed to study the lateral stability of the wheelset on the track. The equation of motion of a two degree of freedom single suspended wheelset model was derived completely. It was found that as the forward velocity of the wheelset increases, the wheelset becomes unstable on the track due to increasing lateral oscillations. These oscillations are limited by flange contact. This novel approach to modelling and simulation of the dynamic behaviour of rail-wheel interface will be useful in the development of intelligent infrastructure diagnostic and condition monitoring systems.

## REFERENCES

- [1] W. Yan, and F. D. Fischer, "Applicability of Hertz Contact theory to rail-wheel contact problems," *Archive of Applied Mechanics*, vol. 70, May 1999, pp. 255–268.
- [2] J. B. Ayasse, and H. Chollet, "Determination of wheel-rail contact patch in semi-Hertzian Conditions", *Vehicle System Dynamics*, vol. 2, Oxford: Number 2, March 2005, pp. 161 – 172.
- [3] X Quost, M. S. A. Eddhahak, J.B. Ayasse, H. Chollet, and P.E. Gautier, "Assessment of the semi-Hertzian method for the determination of the wheel-rail contact patch," *Vehicle System Dynamics*, vol. 44, No. 10, October 2006, pp. 789–814.
- [4] J.J. Kalker, "Rolling contact Phenomena: Linear Elasticity," *CISM International Centre for Mechanical Series*, No. 41, Vol. 6, 2000, 394 pages.
- [5] T. Telliskivi, and U. Olofsson, "Contact mechanics analysis of measured wheel-rail profiles using the finite element method," *Proc. Instn. Mech. Engrs*. Vol. 215, Part F, August 2000.
- [6] J.J. Kalker. "Wheel-rail rolling contact theory," *Wear*, Vol. 144, (1991), pp. 243 – 261.
- [7] J.J. Kalker, "Three dimensional Elastic bodies in rolling contact, Kluwer Academic Publishers, Dordrecht, Boston/London.
- [8] A. Shabana, A., K. Zaazaa, H. Sugiyama, "Railroad Vehicle Dynamics: A Computational Approach," CRC Press, Taylor and Francis Group.
- [9] S. Iwnicki, "Simulation of Wheel-rail contact forces," *Fatigue and fracture of engineering materials and Structures*, Vol. 26, No. 10, 2003, pp. 887-900.
- [10] J. Pombo, J. Ambrosio, M. Silva, "A new wheel-rail contact model for railway dynamics," *Vehicle System dynamics*, Vol. 45, No. 2, February 2007, pp. 165 – 189.
- [11] A. H. Wickens, "The Dynamics of Railway Vehicles Straight Track: Fundamental considerations for lateral stability". *Proceedings, Institute of Mech. Engineers*, Vol. 180, Pt 3F. 1965 pp 1 – 16.
- [12] S. H. Lee, and Y.C. Cheng, "A New Dynamic Model of High Speed Railway Vehicle Moving on Curved Tracks," *Journal of Vibration and Acoustics*, Vol. 130, 2008.
- [13] A. Jaschinski, H. Chollet S.D. Iwnicki, A.H. Wickens and J. Von Würzen, "The Application of Roller Rigs to Railway Vehicle Dynamics," *Vehicle System Dynamics*, Vol. 31, 1999, pp. 345 – 392
- [14] E. Magrab, S. Azaram, B. Balachandran, J. Duncan, and K. Herold, "A Engineers Guide to Matlab," Prentice Hall, 1<sup>st</sup> Ed. August 2000, 512 pages.
- [15] R. Burden, and J. D. Faires, "Numerical Analysis," Thompson Brooks Cole, 8<sup>th</sup> Edition, 2005, 837 pages.